FATIGUE CRACK PROPAGATION OF LASER WELDED BUTT JOINTS

A. Minagi [1] and K. Tokaji [2]

[1] Department of Mechanical Engineering, Osaka Prefectural College of Technology,
26-12 Saiwai-cho, Neyagawa 572-8572, Japan
[2] Department of Mechanical and Systems Engineering, Faculty of Engineering, Gifu University,
1-1 Yanagido, Gifu 501-1193, Japan

ABSTRACT

Fatigue crack propagation (FCP) has been studied using CT specimens cut from laser welded butt joints coupled with two different steels, cold rolled low carbon steel (SP) and high tensile strength steel (HT). When the FCP direction was parallel to the weld line, the FCP rates of the welded specimens characterized in terms of the effective stress intensity factor range were nearly identical to those for the base steel (SP). This indicated that the weld bead had the same intrinsic FCP resistance as the base steel. When the FCP direction was normal to the weld line, FCP rates were decreased temporarily in the weld zone. The decrease of FCP rate still existed after allowing for crack closure and was also seen in FCP behaviour of the specimens subjected to stress-relief annealing and in crack closure-free FCP behaviour at a high stress ratio. It was found that typical fracture mechanism of the welded specimens was the mixed mode of intergranular and transgranular fracture in SP plate, while transgranular fracture mode in the weld zone and in HT plate.

INTRODUCTION

Laser welding is expected to be employed not only for various automotive components but also for extensive applications in other industrial fields, because of advantages such as high power capability, high speed welding, narrow bead width, great precision and low heat distortion. Fatigue performance is very often critical for welded joints in actual service, thus several studies have been reported on the fatigue strength of laser welded lap joints [1-4], but there have been very limited studies on laser welded butt joints [5]. The authors have studied the fatigue strength of laser welded butt joints and indicated that the fatigue strength decreased compared with the unwelded base steel regardless of type of steels and plate thickness coupled [6]. Fatigue crack propagation (FCP) is another important property for welded joints, because most of their fatigue life is often dominated by FCP. However, only a few studies have been reported on the FCP behaviour of laser welded butt joints [7-9].

In the present study, FCP experiments were conducted using two series of laser welded butt joints prepared with the coupling of two different steels. FCP rates in two different directions, *i.e.* parallel and normal to the weld line, were determined. Based on material property changes around the weld zone resulting from welding, crack closure measurements, fracture surface examination and additional FCP experiments, the effect of laser welding on FCP behaviour and the FCP mechanisms are discussed.

EXPERIMENTAL DETAILS

Specimen Preparation

The materials used in the present study are cold rolled low carbon steel (JIS SPCC, designated SP hereafter) and high tensile strength steel (JIS APFC390, HT) with a plate thickness of 2mm. CT specimens employed are shown in Fig.1, which were cut from fatigue specimens with 40mm width used in a previous report [6]. FCP rates for two different directions, *i.e.* parallel and normal to the weld line, were determined, which are referred to as parallel type (P) and normal type (N), respectively. As shown in Table 1, the welded specimens are denoted as SP-P, HT-P, SP-N and HT-N for the combinations of two different steels and FCP directions. Welding was performed by CO_2 laser and the conditions are laser power: 5kW, welding speed: 0.42m/s, focus: surface, shielding gas: Ar $5 \cdot 10^{-4} m^3/s$.

Procedures

Experiments were conducted on a 5kN capacity electro servohydraulic fatigue testing machine operating at a frequency of 30Hz. After introducing a precrack of 2mm long, increasing stress intensity factor range, $\otimes K$, tests were performed at a stress ratio, R, of 0.05 in laboratory air at ambient temperature. Crack closure was measured by a compliance method. Additional experiments were carried out at a high R of 0.7 to obtain crack closure-free FCP behaviour and also performed at R=0.05 using annealed specimens. Crack length was monitored by a travelling microscope with a resolution of 10⌠m.

Residual stress normal to the FCP direction was measured on both surfaces of the welded specimens by X-ray diffraction method. In P-type specimens, measurements were made at the locations of 5mm distance from

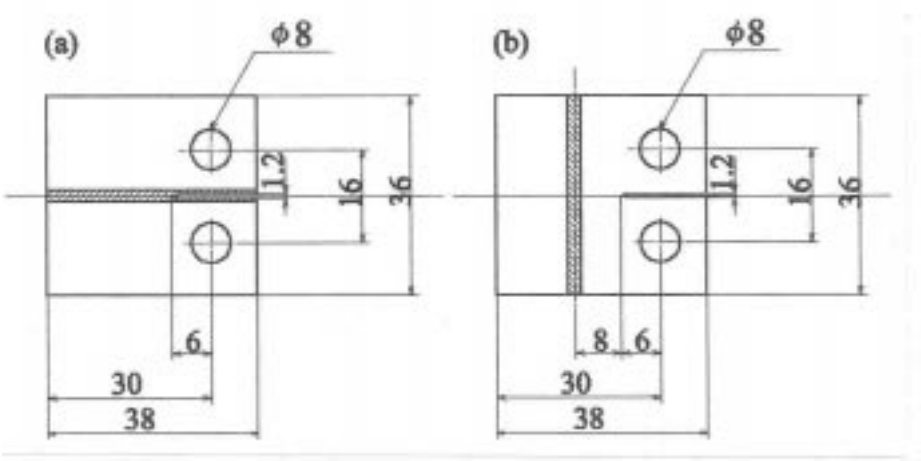

Figure 1: Specimen configurations: (a) parallel type, (b) normal type.

TABLE 1
COMBINATIONS OF STEEL AND FCP DIRECTION.

Specimen code	Steel	FCP direction
SP-P	SP+SP	Parallel
HT-P	SP+HT	Parallel
SP-N	SP+SP	Normal
HT-N	SP+HT	Normal

the centre-line of the weld zone, while in N-type specimens, on the extension of the notch root.

RESULTS

Residual Stress Distribution

Residual stress distributions are shown in Fig.2. In P-type specimens (Fig.2(a)), compressive residual stresses exist regardless of type of steels coupled and HT-P has a slightly larger compressive residual stress than SP-P. In N-type specimens (Fig.2(b)), the hatched region represents the weld zone in which hardness was increased compared with the base steels. Tensile residual stresses are detected around the weld zone in both specimens and large compressive residual stresses exist in SP plate of HT-N.

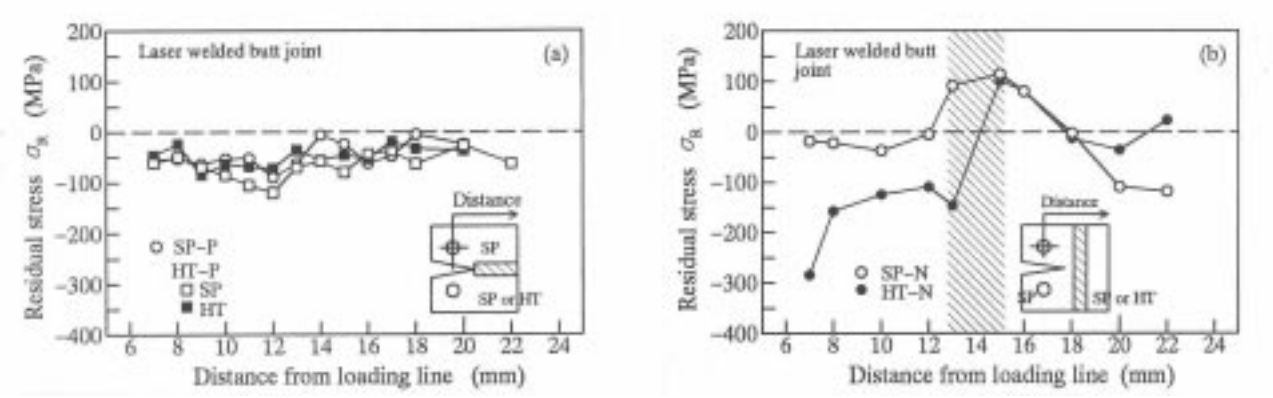

Figure 2: Residual stress distributions: (a) parallel type, (b) normal type.

FCP Behaviour at R=0.05

The relationships between FCP rate, d*a*/d*N*, and stress intensity factor range, ⊗*K*, are shown in Fig.3(a) and (b) for P-type and N-type specimens, respectively. Also included is the FCP behaviour for the unwelded base steel (SP-BASE) for comparison. The FCP rates for SP-P are slightly lower or higher in intermediate or high ⊗*K* regions respectively, than those for the base steel, but the differences are small, thus SP-P seems to have the same apparent FCP resistance as the base steel. On the contrary, HT-P exhibits considerably lower FCP rates compared with the base steel in the entire ⊗*K* region.

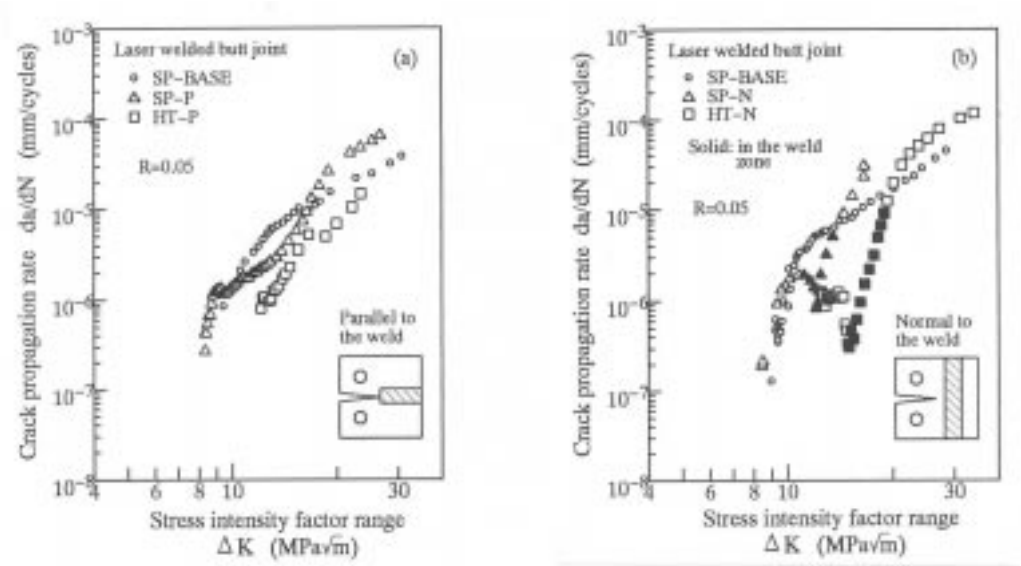

Figure 3: Relationships between FCP rate and stress intensity factor range at *R*=0.05:
(a) parallel type, (b) normal type.

In N-type specimens, when cracks approach to the weld zone, FCP rates decrease gradually, reach the

minimum and then increase within the weld zone, and eventually recover the same rates as the base steel, as indicated by solid symbols in Fig.3(b). Such a temporary decrease of FCP rate was also observed in steel and titanium alloy laser welds by L.W.Tsay et al. [8] and L.W.Tsay and C.Y.Tsay [9], respectively.

FCP Behaviour after Allowing for Crack Closure

Crack closure level, K_{op}/K_{max}, is represented in Fig.4 as a function of K_{max}, where K_{op} and K_{max} are the crack opening and maximum stress intensity factors, respectively. SP-P shows nearly the same crack closure levels as the base steel, while the crack closure levels for HT-P are significantly higher than those for the base steel. Note that SP-N and HT-N exhibit higher crack closure levels within the weld zone.

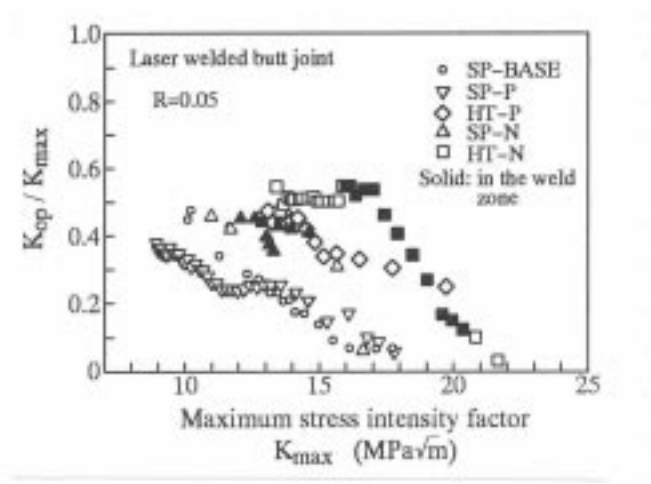

Figure 4: Crack closure behaviour.

Figure 5 shows the FCP data of the welded specimens characterized in terms of the effective stress intensity factor range, $\otimes K_{eff}$. In P-type specimens (Fig.5(a)), the difference in FCP rate between SP-P and HT-P seen in Fig.3(a) completely disappears and both specimens show the same FCP behaviour, indicating that the higher apparent FCP resistance of HT-P is attributed to crack closure. Furthermore, the FCP behaviour of both specimens seems to be similar to that of the base steel because of a negligible difference in FCP rate. As can be seen in Fig.5(b), although the extent of the decrease of FCP rate in the weld zone for SP-N and HT-N is clearly reduced by taking into account crack closure, the decrease of FCP rate is still seen. This suggests that crack closure played a significant role in the decrease of FCP rate in the weld zone, but other factors should also be considered.

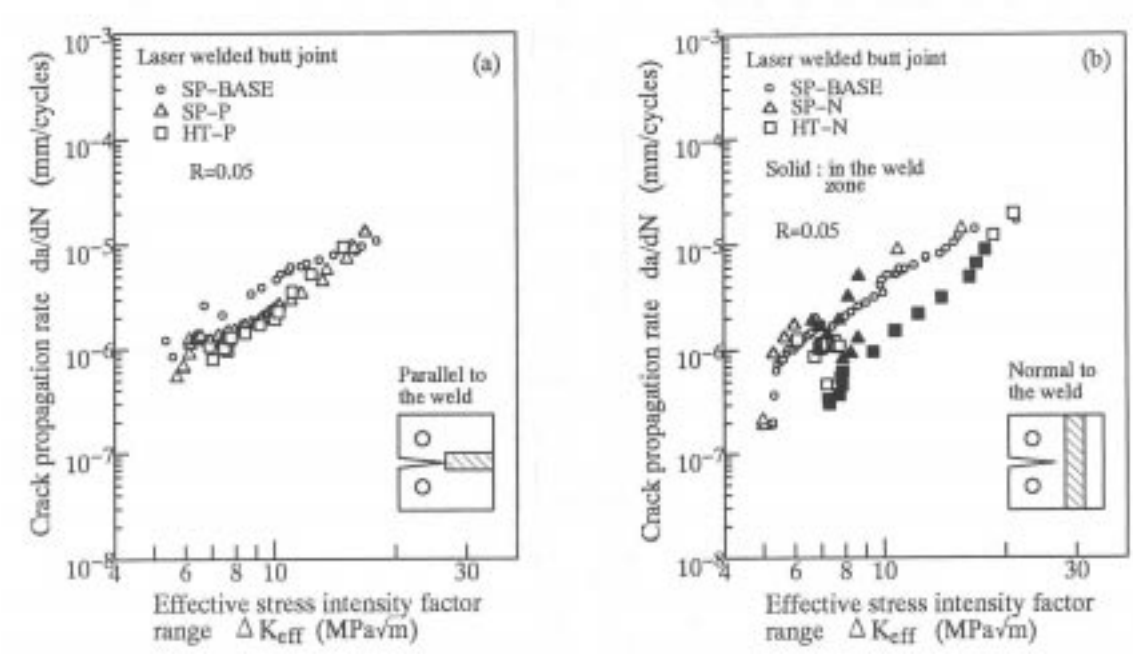

Figure 5: Relationships between FCP rate and effective stress intensity factor range at R=0.05: (a) parallel type, (b) normal type.

FCP Behaviour at R=0.7

FCP experiments were conducted at a high R of 0.7 to obtain crack closure-free FCP behaviour and the obtained results are represented in Fig.6. In P-type specimens (Fig.6(a)), the FCP rates for both specimens, SP-P and HT-P, are identical independent of type of steels coupled and both specimens exhibit the same FCPbehaviour as the base steel, indicating that the weld zone has the same intrinsic FCP resistance as the base steel. In N-type specimens (Fig.6(b)), the FCP behaviour is basically similar to the FCP behaviour after allowing for crack closure shown in Fig.5(b) and the decrease of FCP rate can be seen in the weld zone, but the extent is clearly reduced compared with the data at R=0.05. This result also confirms that other factors than crack closure exert an influence on the decrease of FCP rate in the weld zone.

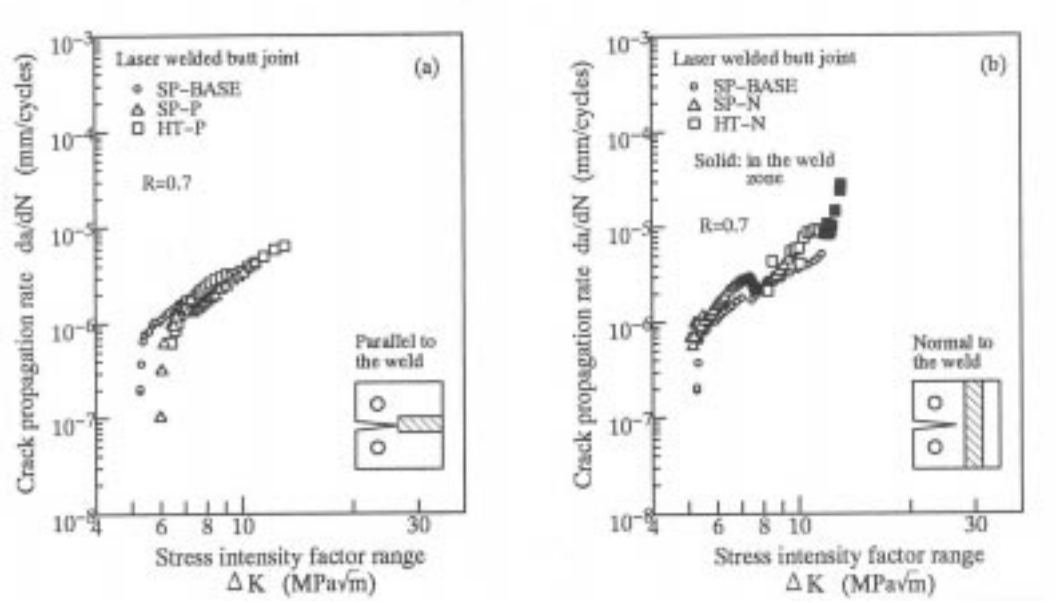

Figure 6: Relationships between FCP rate and stress intensity factor range at R=0.7: (a) parallel type, (b) normal type.

FCP Behaviour of Annealed Specimens

FCP rates for SP-N(SA) and HT-N(SA) subjected to stress-relief annealing at 600□ for 1h in vacuum are demonstrated in Fig.7(a) as a function of ⊗K. Both specimens show a decrease of FCP rate in the weld zone. Figure 7(b) represents the FCP data characterized in terms of ⊗K_{eff}. Note that the decrease of FCP rate in the weld zone is still seen in both specimens. Therefore, the FCP behaviour of the annealed specimens is

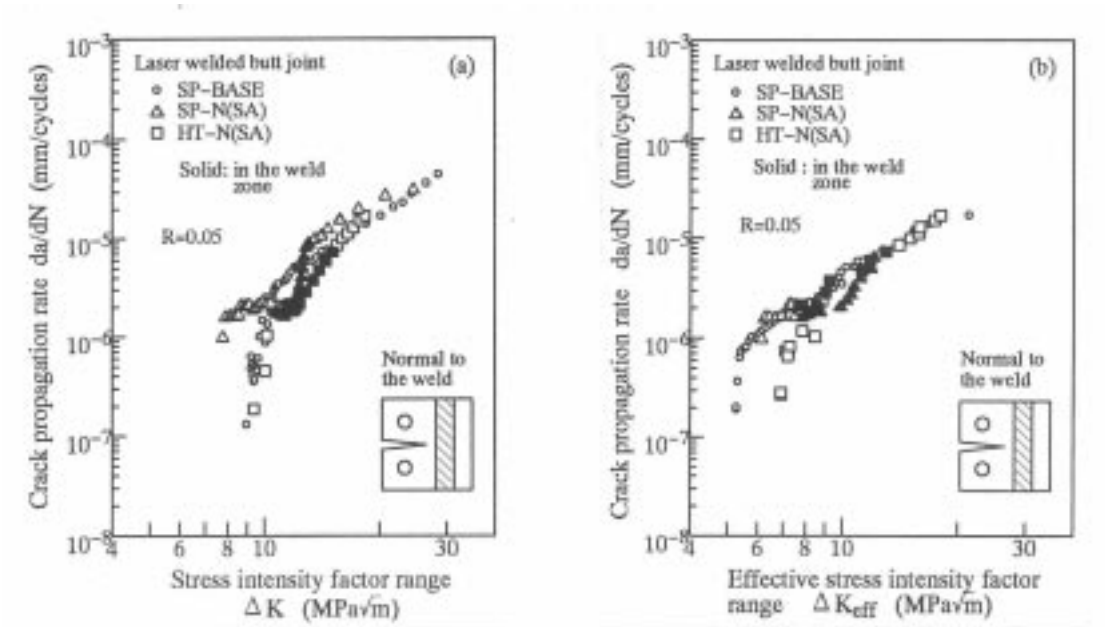

Figure 7: FCP behaviour at R=0.05 in annealed specimens characterized in terms of (a) stress intensity factor range, (b) effective stress intensity factor range.

basically the same as that of the as-welded specimens, indicating that residual stress is not responsible for the decrease of FCP rate in the weld zone.

Fractography

SEM examination of fracture surfaces in the base steel (SP-BASE) revealed that predominant fracture mode was ductile transgranular regardless of $\otimes K$. At R=0.05, cracks in P-type specimens, SP-P and HT- P, initially grew in the weld bead, but deviated gradually after a certain distance and thereafter grew in the heat affected zone (HAZ) (SP plate side in HT-P). The fracture surface appearances are represented in Fig.8, showing that the fracture mode is transgranular in the weld bead, while transgranular with a large fraction of intergranular fracture in HAZ. At R=0.7, cracks grew in the weld bead and the fracture mode was transgranular regardless of $\otimes K$.

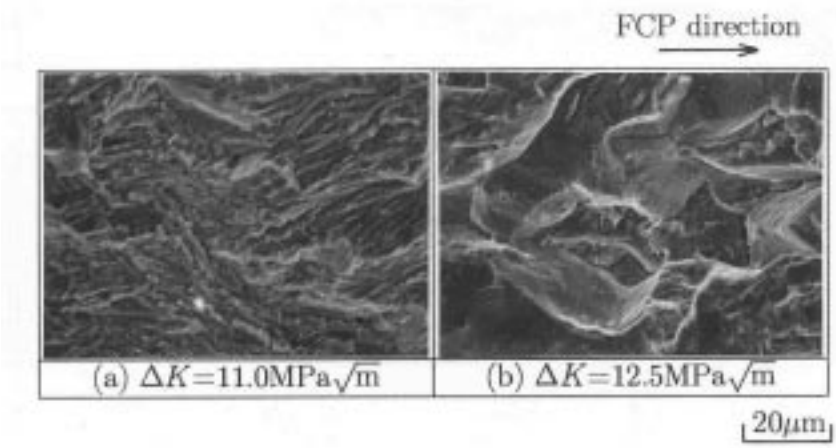

Figure 8: SEM micrographs of fracture surfaces in a parallel type specimen, SP-P, (R=0.05): (a) weld bead, (b) heat affected zone (HAZ).

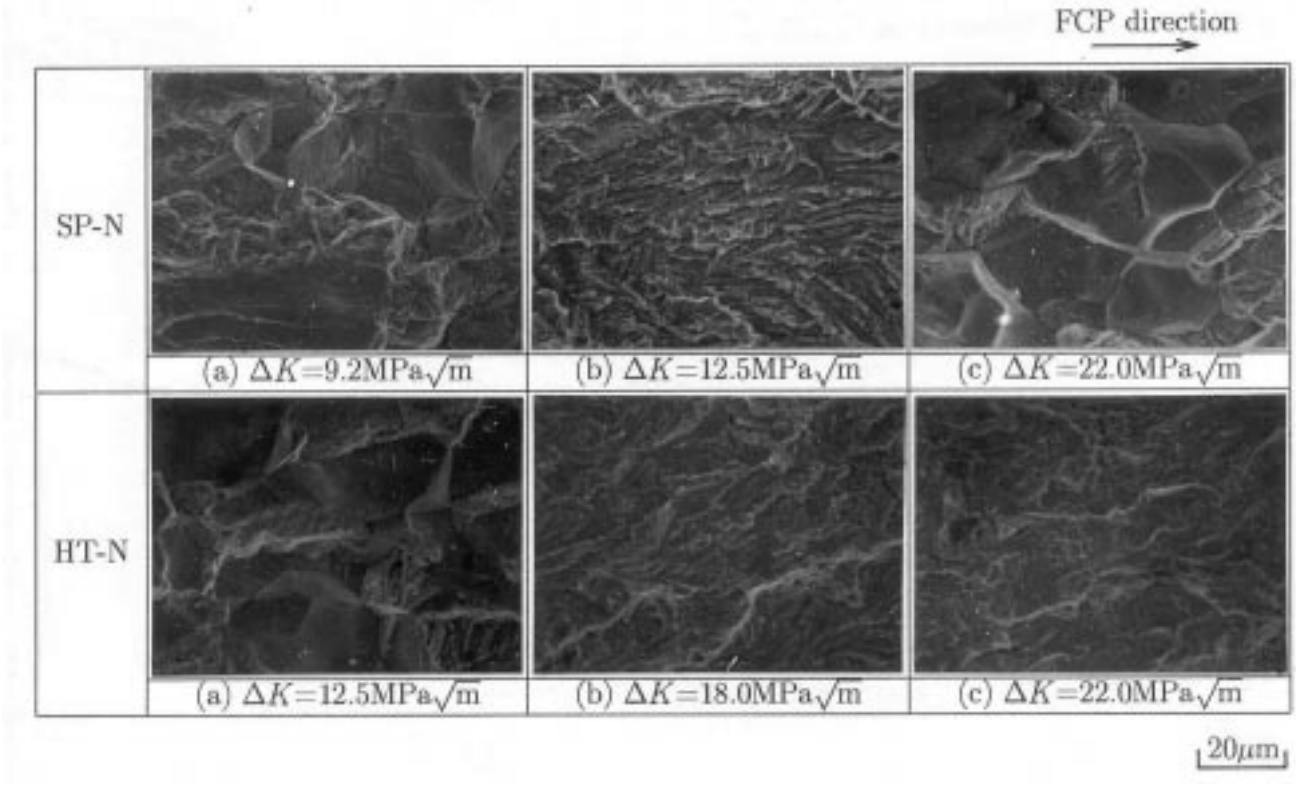

Figure 9: SEM micrographs of fracture surfaces in as-welded normal type specimens (R=0.05): (a), (b) and (c) are fracture surfaces in SP plate, in weld zone and in SP or HT plate, respectively.

Figure 9 shows SEM micrographs of fracture surfaces in the as-welded N-type specimens, where (a), (b) and (c) indicate fracture surfaces in SP plate before cracks reach the weld zone, in the weld zone, and in SP plate or HT plate after cracks grew across the weld zone, respectively. In SP-N, ductile transgranular fracture is predominant mode in the weld zone, but mixed mode of transgranular and intergranular fracture can be seen in SP plate. On the contrary, HT-N reveals mixed mode of transgranular and intergranular fracture in SP plate, while transgranular fracture in the weld zone and in HT plate. The same features were confirmed in the

annealed specimens and in the as-welded specimens at R=0.7.

Figure 10 shows the fraction of intergranular fracture as a function of crack length in all N-type specimens tested, where the hatched area in the figure represents the weld zone. As shown in Fig.9, no intergranular fracture is seen in the weld zone and in HT plate, while a relatively large fraction of intergranular fracture is observed in SP plate.

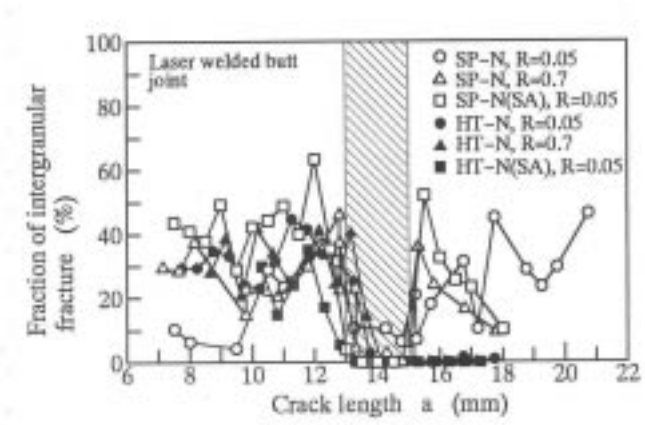

Figure 10: Fraction of intergranular fracture as a function of crack length in normal type specimens.

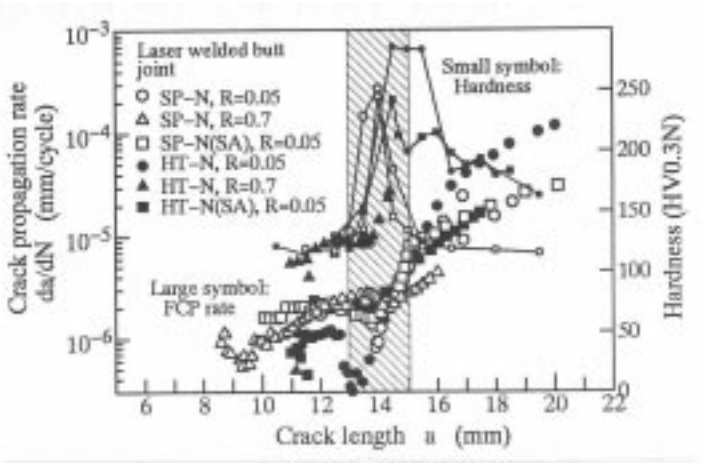

Figure 11: Changes in FCP rate and hardness with crack length in normal type specimens.

DISCUSSION

FCP Resistance Parallel to the Weld Line

After allowing for crack closure, the FCP behaviour of P-type specimens was identical independent of type of steels coupled, which was also the same as that of the base steel. In addition, this was confirmed in crack closure-free FCP behaviour obtained at a high stress ratio. Therefore, the difference in apparent FCP resistance seen in Fig.3(a) may be attributed to crack closure induced by residual stress and thus it is concluded that the weld bead has the same intrinsic FCP resistance as the base steel.

FCP Resistance Normal to the Weld Line

As shown in Fig.2(b), tensile residual stresses existed around the weld zone and the FCP behaviour of the annealed specimens was basically the same as that of the as-welded specimens. These results clearly indicate that residual stress is not responsible for the decrease of FCP rate in the weld zone. Furthermore, the decrease of FCP rate was still seen in the FCP behaviour after allowing for crack closure and in the crack closure-free FCP behaviour at R=0.7. Therefore, other factors than crack closure should be considered in explaining the decrease of FCP rate in the weld zone.

Figure 11 shows the changes in FCP rate and hardness as a function of crack length. As described previously, the decrease of FCP rate is seen in the weld zone, which corresponds to the increase in hardness. Therefore, it is assumed that the actual driving force at the crack tip would be reduced when cracks grow within the weld zone, because the plastic zone size at the crack tip becomes small due to the increase of yield stress with increasing hardness.

The decrease of FCP rate in the weld zone might be attributed to the sudden change in fracture mechanism from the mixed mode of transgranular and intergranular fracture to the transgranular fracture mode. However, it does not appear to be the cause for the decrease of FCP rate, because FCP rates of SP plate with intergranular fracture mode were almost the same as those of the base steel (SP) with transgranular fracture mode, indicating that FCP rates are insensitive to the change in fracture mechanism.

It should be emphasized that intergranular fracture was seen only in SP plate of the welded specimens. No intergranular fracture was observed in the unwelded base steel (SP), thus it was thought that SP plate of the

welded specimens was thermally affected by laser welding. EPMA analyses were performed to examine segregation at or near grain boundaries. However, neither segregation of any particular elements nor foreign elements were not detected. FCP experiments were conducted using the welded specimens subjected to full annealing at 910□. The obtained results showed that the decrease of FCP rate in the weld zone completely disappeared and no intergranular fracture was seen in SP plate. This result indicates indirectly that segregated elements re-dissolved within grains due to the higher temperature annealing.

CONCLUSIONS

(1) In the FCP direction parallel to the weld line, the FCP rates of the welded joints coupled with the same steel were the same as those of the base steel, while the welded joints coupled with different steels showed lower FCP rates than the base steel in the entire $\otimes K$ region. After allowing for crack closure and in crack closure-free FCP behaviour at a high stress ratio, the welded specimens showed the same FCP rates as the base steel regardless of type of steels coupled.

(2) In the FCP direction normal to the weld line, FCP rates decreased gradually when cracks approached to the weld zone, reached the minimum and then increased in the weld zone, regardless of type of steels coupled. This decrease of FCP rate still existed after allowing for crack closure.

(3) The decrease of FCP rate in the weld zone was also seen in the FCP behaviour of the specimens subjected to stress-relief annealing and in the crack closure-free FCP behaviour at a high stress ratio.

(4) In the welded specimens, mixed mode of transgranular and intergranular fracture was seen in SP plate, while transgranular fracture mode in the weld zone and in HT plate.

(5) The decrease of FCP rate and intergranular fracture completely disappeared in the welded specimens subjected to full annealing.

ACKNOWLEDGEMENTS

The authors wish to thank Marujun Co. Ltd. for providing the test materials. Thanks are also due to Research Institute of Industrial Products Technology, Gifu, for assistance with EPMA analyses.

REFERENCES

1. Hsu. C. and Albright, C.E. (1991) *Engng Fract. Mech.* **39**, 575.
2. Wang, P.-C. and Ewing, K.-M. (1991) *Welding Journal* **43,** 43.
3. Flavenot, J.-F., Deville, J.-P., Diboine, A., Cantello, M. and Gobbi, S.-L. (1993) *Weld World* **31**, 358.
4. Wang, P.C. (1995) *Int. J. Fatigue* **17**, 25.
5. Guglielmino, E., Rosa, G.La., Oliverri, S.M. and Pasta, A. (1993) *Proc. 1st. Sympo. Automo. Tech. Automa*. **26,** 57.
6. Tokaji, K., Shiota, H., Minagi, A. and Miyata, M. (1999) *Proc. Inter. Conf. Adv. Tech. Experi. Mech*. **2**, 710.
7. Hwang, J.R., Doong J.L. and Chen, C.C. (1996) *Materials Transactions, JIM* **37**, 1443.
8. Tsay, L.W., Chung, C.S. and Chen, C. (1997) *Int. J. Fatigue* **19**, 25.
9. Tsay, L.W. and Tsay, C.Y. (1997) *Int. J. Fatigue* **19**, 713.